



# COMPARATIVE EVALUATION OF SENSITIVITY OF WELDED JOINTS ON ALLOY INCONEL 690 TO HOT CRACKING

K.A. YUSHCHENKO, V.S. SAVCHENKO, N.O. CHERVYAKOV, A.V. ZVYAGINTSEVA,  
G.G. MONKO and V.A. PESTOV

E.O. Paton Electric Welding Institute, NASU, Kiev, Ukraine

Sensitivity of metal of the welds made with wires Inconel® 52 and Inconel® 52MSS to hot cracking was evaluated. The machine testing methods (Varestraint-Test and PVR-Test), which provide for forced deformation of test specimens during welding, were used. The welds made with wire Inconel 52MSS were shown to be more resistant to ductility dip cracking, but several times more sensitive to solidification cracking. Evaluation of ductile properties of the weld metal using the «Ala-Too» machine showed that the Inconel 52MSS type weld metal had no ductility dip, whereas the Inconel 52 type weld metal was characterized by a pronounced decrease in the elongation values.

**Keywords:** TIG welding, nickel alloys, filler wire, weld metal, evaluation of crack resistance, ductility dip range, grain boundary, forced deformation

Welded joints on high-alloy steels with a stable austenitic structure and nickel alloys are known to be characterised by high sensitivity to hot cracking during fusion welding. As to their nature, hot cracks can be subdivided into two types (Figure 1): solidification (type 1) and underbead (type 2) cracks that form in the process of thermal-force loading of the multi-pass weld metal zones [1]. The temperature range of formation of the solidification cracks depends on the range of the solid-liquid state of metal during solidification of the weld. The lower limit of this range is determined by the value of solidus temperature at the end of solidification,  $T_S$ . The ductility dip temperature range is determined by an approximate ratio of  $(0.6-0.8)T_S$  [2]. In this range the cracks initiate and propagate along the boundaries of high-angle austenitic grains [3].

The sensitivity to hot cracking is determined by the following factors [4-8]:

- chemical composition of the weld metal in terms of the content of main and impurity elements, having

a limited solubility in solid solution and determining the solidification temperature range;

- value and rate of the growth of strain in solidification of the weld and its subsequent cooling;

- presence of conditions for redistribution of impurity elements, such as carbon, sulphur, oxygen etc., characterised by a high diffusivity under the thermal-force impact on metal by the fusion welding process;

- formation of the fine weld structure in one- and multi-pass welding, which determines the process of plastic deformation in metal of the polycrystalline welds;

- cohesive strength of grain boundaries in the welds with a stable austenitic structure, which determines conditions for initiation of hot cracks.

The purpose of this study was to perform comparative evaluation and investigation of the sensitivity of welds and welded joints on alloy Inconel 690 made by using welding wires Inconel 52 and Inconel 52MSS to hot cracking.

Special specimens are available for simulation of conditions of deformation of the deposited metal in multi-pass welding of real structures. Evaluation of the sensitivity to hot cracking, including in the multi-pass welds, is performed on the test specimens simulating the thermal-force impact exerted by the welding process on formation of the weld structure and initiation of hot cracks. Also, the use is made of the machine testing methods with the graduated forced deformation. In this case the most efficient methods are Varestraint-Test and PVR-Test (Programmierter Verformungs-Riss Test) [9]. So, these methods were employed to evaluate the sensitivity to solidification cracking, as well as to ductility-dip cracking in multi-pass welding of nickel alloy Inconel 690 by using welding wire Inconel 52MSS characterised, according to the preliminary data, by high crack resistance in the low-temperature ductility dip range. Investiga-

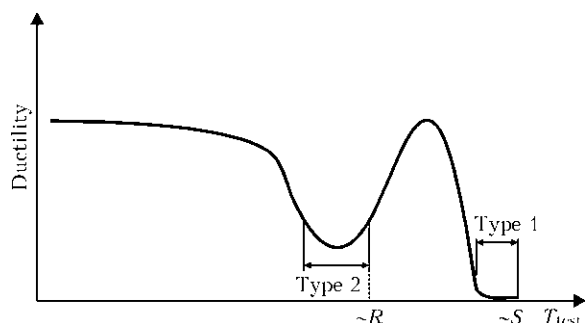


**Figure 1.** Temperature ranges in which low ductility leads to formation of two types of the cracks during welding [1]:  $S$  — solidus;  $R$  — recrystallisation

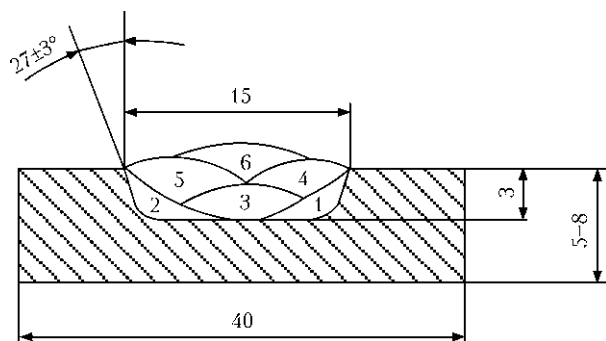


**Figure 2.** Schematic of filling of the groove with beads (deposition welds) in test specimens according to the Varestraint-Test and PVR-Test procedures

tions provided for plotting of brittle temperature ranges and determination of the critical value of strain  $\varepsilon_{cr}$  in fusion welding. In addition, the critical deformation rate was determined (PVR-Test), thus allowing evaluation of the sensitivity to formation of both solidification and ductility-dip cracks.

Chemical composition of the base metal and welding wires is given in the Table.

Microstructure of alloy Inconel 690 is fine-grained, non-textured, and consisting of austenitic grains and annealing twins located inside the grains. No substantial amounts of redundant phases or boundary precipitates was detected.

Specimens for investigation of weldability by the Varestraint-Test and PVR-Test procedures were prepared by making a groove in the Inconel 690 specimens measuring  $8 \times 40 \times 170$  and  $8 \times 50 \times 200$  mm. This groove was preliminarily filled up with a multilayer weld using wires Inconel 52 and Inconel 52MSS. Elements of the edge groove and sequence of deposition of the beads are shown in Figure 2.

Welding was performed by the TIG method in argon atmosphere using 0.9 mm diameter wires Inconel 52 and Inconel 52MSS. The stable weld formation was achieved by weaving the tungsten electrode and filler wire at a preset amplitude and frequency under optimal welding conditions. Test specimens were cut out from the weld-deposited plates: specimens measuring  $170 \times 70 \times 3.5$  mm for Varestraint-Test, and specimens measuring  $200 \times 40 \times 3.5$  mm for PVR-Test. In addition, specimens (Figure 3) for evaluation of ductility of the deposited metal in the ductility dip temperature range were cut out from the weld metal [10].

The machine testing methods with forced deformation of a specimen welded, providing the deformation of a graduated value and rate, hold promise for evaluation of weldability of metallic materials.

Chemical composition of base metal and welding wires Inconel® 52 and Inconel® 52MSS, wt. %

Material	C	Mn	Ni	Cr	Fe	Nb	Mo	Ti	S	P	Al	Si
In 690	0.020	—	Base	29.72	10.30	—	—	0.28	0.002	0.005	0.87	0.32
In 52MSS	0.024	0.29	54.55	30.30	7.24	2.52	3.45	0.25	0.002	0.0055	0.22	0.15
In 52	0.021	0.24	59.17	29.19	9.99	—	0.01	0.51	0.001	0.003	0.72	0.12

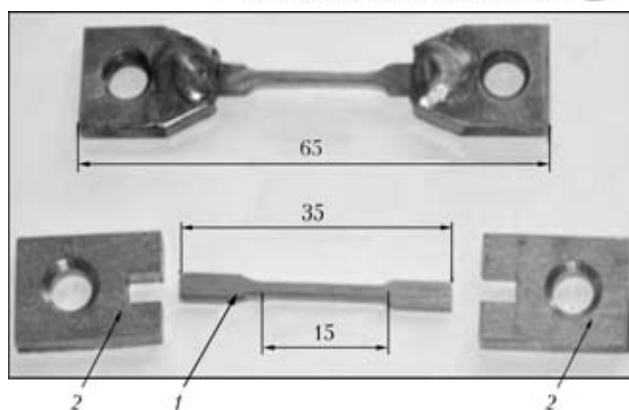


**Figure 3.** Appearance of composite specimen for evaluation of high-temperature properties of multi-pass welds: 1 — gauge section of composite specimen of the Inconel 690 joint made with wires Inconel® 52MSS and Inconel® 52; 2 — grip of 304 type steel

The evaluation method is implemented by performing TIG welding of a flat plate without filler and by simultaneously subjecting this plate to the time-variable deformation in a direction that is longitudinal with respect to the welding direction.

The principle of implementation of the PVR-Test procedure is shown in Figure 4 [11]. A characteristic feature of this procedure is ensuring the required range of the value of the forced deformations of a test specimen during welding and the rate of their variations. In this case it is required that the following two deformation dependences be fulfilled:

$$\frac{\Delta l}{\Delta t} = v, \quad \frac{\Delta v}{\Delta t} = \text{const},$$

where  $l$  is the displacement of grips 2 (see Figure 4);  $v$  is the speed of displacement of the grips; and  $t$  is the time of the displacement.

Critical deformation rate  $v_{cr}$  at which the first cracks form serves as a criterion of the sensitivity to cracking. During welding the cracks may simultaneously form in the weld and in the HAZ metal. These two types of the cracks are of a different nature [12] and, as a rule, form at a different rate of critical deformation  $v_{cr}$ . The solidification cracks are caused by development of the segregation process and formation of intergranular liquid interlayers in a temperature range close to  $T_s$ . They are located along the grain boundaries in the weld metal. The ductility-dip cracks form as a result of a loss of ductility of metal. They are located at some distance from the fusion line in the HAZ metal, the temperature of which has not yet reached the melting temperature. This makes it possible to quantitatively characterise the sensitivity

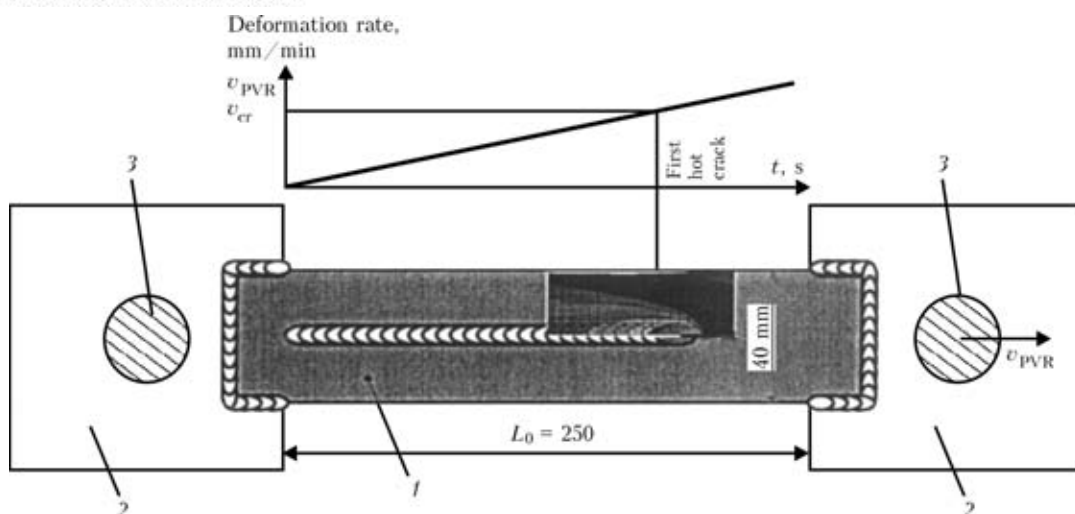


**Figure 4.** Schematic of the principle of implementation of PVR-Test [11]: 1 — specimen; 2 — grips; 3 — fastening pins for loading of specimens

to a certain type of the cracks. Position of a specimen after welding and its surface appearance are shown in Figures 5 and 6.

The diagram of displacement of grips of the PVR-Test machine depending on the time is fixed during an experiment, and the rate of deformation of metal in each of the eight regions is determined based on the diagram data. Such measurements make it possible to plot dependence of the quantity of the investigated type of the cracks on the deformation rate, and determine the value of critical deformation rate  $v_{cr}$  from the plot by way of extrapolation at intersection of the straight line with the abscissa axis.

The quantity of the cracks classified as the ductility-dip ones was counted by choosing the cracks that began and ended in the HAZ metal. This was done by using an optical microscope with  $\times 50$  magnification.

The cracks that formed in the weld were regarded as the solidification ones. Some of them stopped in the HAZ metal by forming a characteristic plastic strain in the stopping location. Analysis of the sensitivity to hot

cracking was carried out by counting the quantity of the ductility-dip cracks located at some distance from the fusion line, as well as the solidification cracks that formed, as a rule, in the reference weld. The scheme accepted for classification of the cracks (Figure 7) was similar to that given in study [13].

Investigation of weldability by the Varestraint-Test procedure was performed by subjecting a metal plate during welding to forced bending deformation. In this case the deformation rate should exceed the welding speed to minimise displacement of the weld pool during the deformation time. Parameters of the brittle temperature range, as well as the critical value of strain  $\epsilon_{cr}$  at which no cracks have yet formed served as a weldability evaluation criterion. Crack resistance of the wires was investigated on a series of plates measuring  $170 \times 60 \times 3.5$  mm. The chosen forced deformation values ranged from 0.2 to 2.0 %, this corresponding to the mandrel radii ranging from 850 to 85 mm. Welding parameters for the Varestraint-Test procedure were as follows:  $I_w = 90$  mm,  $U_a = 9.7$  V,  $v_w = 8$  m/h, and argon flow rate — approximately 8.5 l/min.

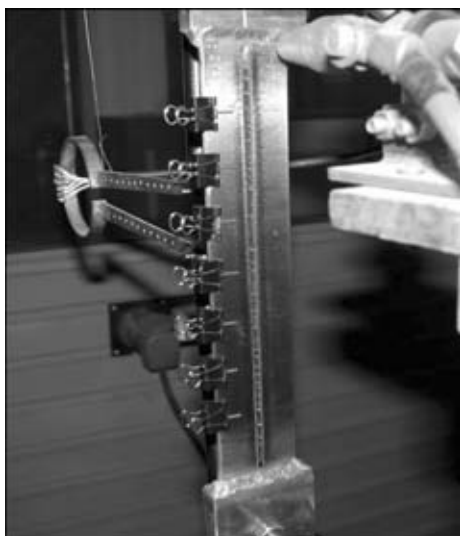


**Figure 5.** General view of specimen after welding using the PVR-Test machine

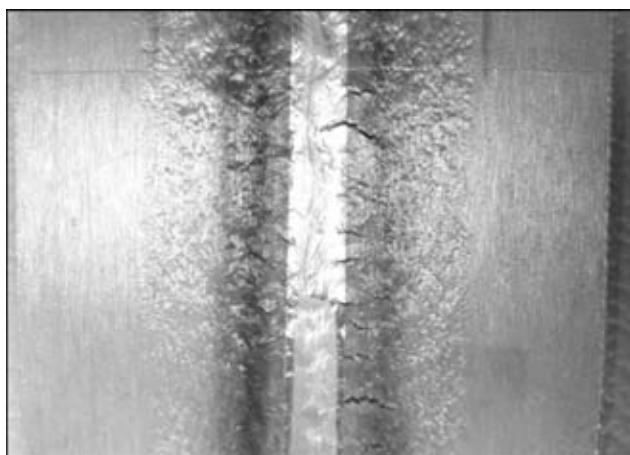


**Figure 6.** Surface of specimen after weldability tests by the PVR-Test procedure

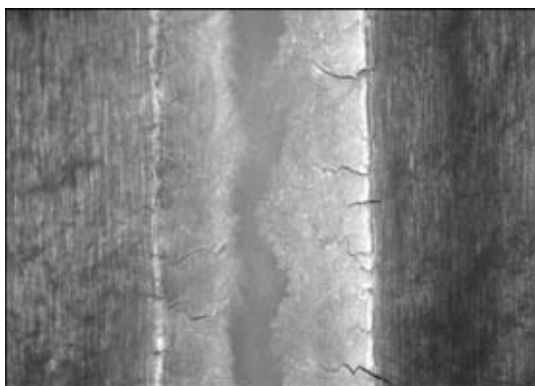


**Figure 7.** Solidification cracks in welds made with wire Inconel® 52MSS (×10)

The tests were conducted to determine the values of tensile strength and elongation  $\delta$  of the investigated metal in a temperature range from 20 to 1100 °C by using the «Ala-Too» testing machine (of the Gleeble type). The software provided maintaining of the preset temperature, fixing of the loading, and calculation and graphical representation of the load-displacement curve.

The loading systems of the «Ala-Too» machine allow evaluation of metal ductility in a wide temperature range in vacuum ( $10^{-5}$  mm Hg) (Figure 8).

The investigation results revealed substantial differences in the sensitivity to solidification and ductility-dip cracking between the weld metals obtained with wires Inconel 52 and Inconel 52MSS. The welds made with wire Inconel 52 had a minimal sensitivity to solidification cracking, and were sensitive to ductility-dip cracking. The ductility-dip cracks were located in regions of the HAZ metal whose temperature during welding did not reach  $T_S$  at a distance of 100  $\mu$ m to 2 mm from the fusion line.

And on the contrary, the welds made with wire Inconel 52MSS were very sensitive to solidification cracking and almost insensitive to ductility-dip cracking. This dependence is schematically shown in Figure 9.

The results obtained were confirmed by the brittle temperature ranges (BTR) plotted by using the

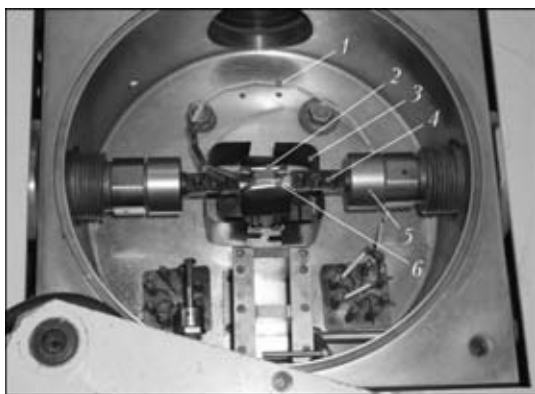


**Figure 8.** Vacuum chamber of the «Ala-Too» machine with device for deformation of specimens: 1 – platinum-rhodium thermocouple; 2 – radiation heating device; 3 – thermal shield; 4 – grip; 5 – draw bar; 6 – specimen

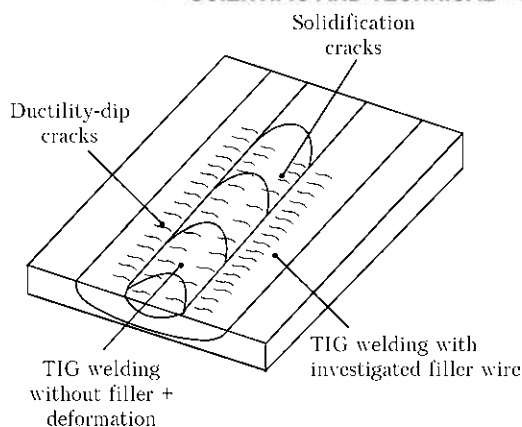


**Figure 9.** Schematic of preferential location of cracks in welds after tests by the PVR-Test procedure

Varestraint-Test procedure (Figure 10). Wire Inconel 52 was shown to have two brittle temperature ranges – high- and low-temperature ranges.

Testing of wire Inconel 52MSS with a forced deformation of up to 2.3 % revealed no low-temperature range, this being indicative of a higher resistance of these welds to ductility-dip cracking.

Microstructure of metal of the investigated welds with a face-centred cubic lattice was polycrystalline, consisting of grains of a different crystallographic orientation within each grain, separated by boundaries. Hot cracks, and first of all the ductility-dip cracks, may form along the grain boundaries under the corresponding conditions. According to the solidification conditions, the welds had either a directed cellular or cellular-dendritic structure, determining the mechanism of formation of the solidification cracks. The ductility dip temperature range was present in the Inconel 52 welds and absent in the Inconel 52MSS welds over the entire range of the deformations applied.

Based on the results obtained, it can be considered that the solidification cracks initiate mainly along the high-angle boundaries of elongated austenitic grains in the process of their formation during solidification (Figure 11).

Metallographic examinations of the multilayer welds made by TIG welding with filler wire Inconel 52MSS and of the reference weld made by TIG welding

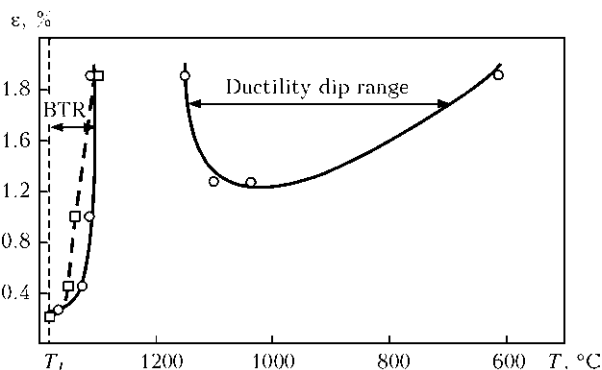


**Figure 10.** Brittle temperature ranges of the welds made with wires Inconel® 52 (solid line) and Inconel® 52MSS (dashed) in evaluation of weldability by the Varestraint-Test procedure

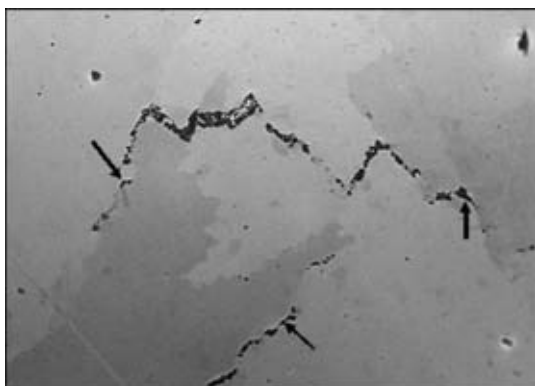


**Figure 11.** Character of propagation of solidification cracks (indicated by arrows) in weld metal obtained with wire Inconel® 52MSS ( $\times 200$ )

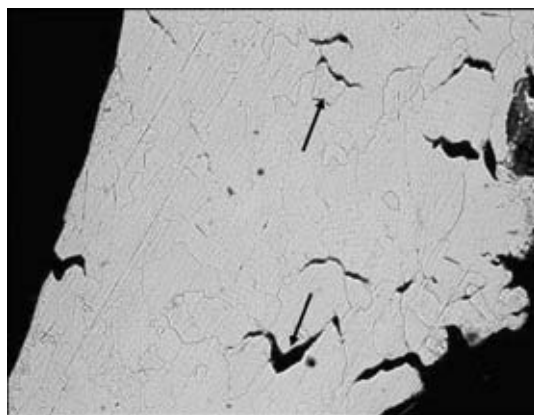


**Figure 13.** Microstructure ( $\times 100$ ) of metal of the multi-pass weld made with wire Inconel® 52 at ductility dip temperature (intergranular fracture is shown by arrows)

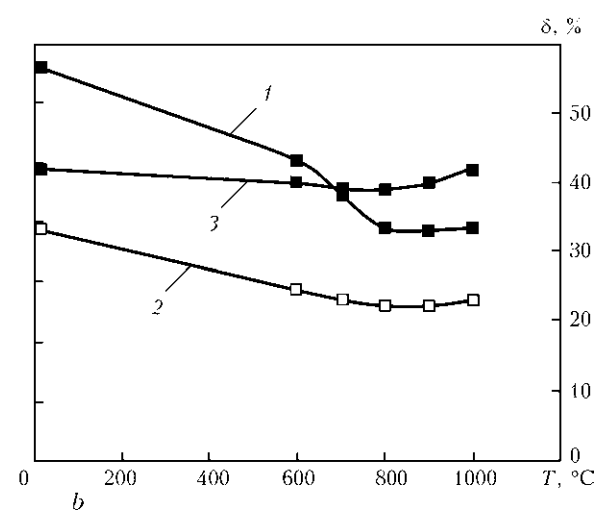
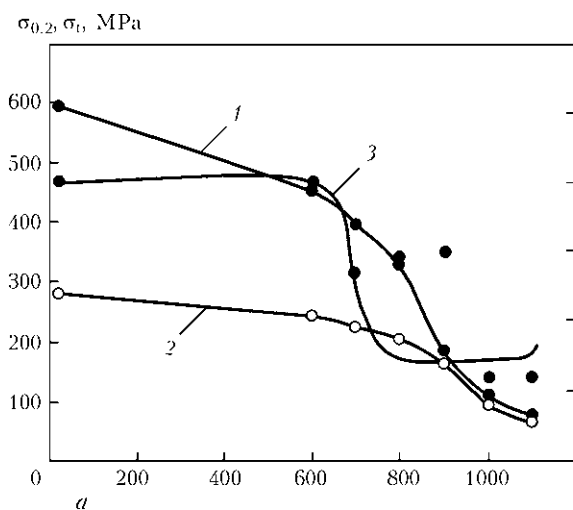


**Figure 12.** Temperature dependence of strength and ductility of specimens of the welded joint made with wires Inconel® 52 (*a*) and Inconel® 52MSS (*b*): 1 –  $\sigma_t$ ; 2 –  $\sigma_{0.2}$ ; 3 –  $\delta$

without filler during the forced deformation by the PVR-Test procedure confirmed the data that metal of the investigated welds is practically insensitive to formation of the ductility-dip cracks, which are the main type of microcracks forming in the multi-pass welds with a stable austenitic structure.

Results of investigation of temperature dependence of ductility of metal of the welds made with wires Inconel 52MSS and Inconel 52 are shown in Figure 12.

In contrast to specimens of the joints welded with wire Inconel 52, the dip in the characteristic temperature range is only slightly discernible in the curve of ductility of the joints welded with wire Inconel 52MSS (Figure 12, *b*), which is attributable to peculiarities of composition of this wire.

Analysis of microstructure of weld metal specimens showed that brittle intergranular fracture occurred in the Inconel 52 welds as a result of loading (Figure 13).

Therefore, the main cause of formation of the ductility-dip cracks in welds with the stable austenitic structure is migration of a number of impurity elements to grain boundaries in the multi-pass welds, this migration being accelerated by thermoplastic deformation.

Analysis of the published data [15], as well as the obtained investigation results allow putting forward a hypothesis on the probable mechanism of formation of cracks in multi-pass welding of austenitic high-alloy steels and nickel alloys. According to this hypothesis, the cracks form along the high-angle grain boundaries because of segregation of impurity elements, such as carbon, oxygen, sulphur and phosphorus, which actively diffuse to the boundaries [16, 17]. The mechanism of the effect of the impurities on embrittlement of the grain boundaries in the ductility dip temperature range requires additional investigation, which is planned to do in further studies.

## CONCLUSIONS

1. The machine testing methods (Varestraint-Test and PVR-Test) providing for the forced deformation of test specimens during welding, as well as the technological test, i.e. multilayer welding, were used for the investigations.

2. Brittle temperature ranges were plotted for the welds in tests by the Varestraint-Test procedure. It was shown that welding with wire Inconel 52MSS in all shielding atmospheres resulted in formation of only



solidification cracks in the welds. In this case, the critical strain value was  $\varepsilon_{cr} \approx 0.43\%$ . Ductility-dip cracks were absent in all variants of the welds in a temperature range of 700–1000 °C.

3. As shown by using the PVR-Test procedure, the sensitivity to formation of the ductility-dip cracks was very low. At the same time, the solidification cracks were observed in the Inconel 52MSS welds under certain deformation conditions.

4. Evaluation of ductile characteristics of metal of the welds made with the investigated wires using the «Ala-Too» machine showed that the Inconel 52MSS type weld metal had no ductility dip, whereas the Inconel 52 type weld metal was characterised by a pronounced decrease in the elongation values. The data obtained prove a high resistance of the Inconel 52MSS welds to ductility-dip cracking (type 2) and sensitivity to solidification cracking in the brittle temperature range (type 1).

5. The probable cause of intergranular fracture of the welds is decrease in values of cohesive strength of the grain boundaries.

1. Hemsworth, W., Boniszewski, T., Eaton, N.F. (1969) Classification and definition of high temperature welding cracks in alloys. *Metal Constr. and British Welding J.*, **1**, 25, 5–16.
2. Torres, E.A., Peternella, F.G., Caram, R. et al. (2010) In situ scanning electron microscopy high temperature deformation experiments to study ductility dip cracking of Ni–Cr–Fe alloys. In: *In situ studies with phonons, neutrons and scattering*. Berlin; Heidelberg: Springer, 27–39.
3. Lippold, J.C., Kotecki, D.J. (2005) *Welding metallurgy and weldability of stainless steels*. John Wiley & Sons.
4. Collins, M.G., Lippold, J.C. (2003) An investigation of ductility dip cracking in nickel-based weld metals. Pt I. *Welding J.*, **82**(10), 288–295.
5. Collins, M.G., Ramirez, A.J., Lippold, J.C. (2003) An investigation of ductility dip cracking in nickel-based weld metals. Pt II. *Ibid.*, **82**(10), 348–354.
6. Collins, M.G., Ramirez, A.J., Lippold, J.C. (2004) An investigation of ductility dip cracking in nickel-based weld metals. Pt III. *Ibid.*, **83**(2), 39–49.
7. Lippold, J.C., Nissley, N.E. (2007) Further investigation of ductility dip cracking in high chromium, nickel-based filler metals. *Welding in the World*, **51**(9/10), 24–30.
8. Noecker, F.F., DuPont, J.N. (2009) Metallurgical investigation into ductility dip cracking in nickel-based alloys. Pt II. *Welding J.*, **88**(3), 62–77.
9. Cross, C.E., Coniglio, N. (2008) Weld solidification cracking: critical conditions for crack initiation and growth. In: *Hot cracking phenomena in welds II*. Berlin; Heidelberg: Springer.
10. Zvyagintseva, A.V., Yushchenko, K.A., Savchenko, V.S. (2001) Effect of structural changes in high-temperature heating on ductile characteristics of nickel alloys. *The Paton Welding J.*, **4**, 13–17.
11. Herold, H., Hubner, A., Zinke, M. (2004) Investigation of the use of nitrogenous shielding gas in welding and its influence on the hot-crack behaviour of high temperature resistant fully austenitic Ni- and Fe-base alloys. *IIW Doc. IX-2110-04*.
12. Yushchenko, K.A., Savchenko, V.S. (2008) Classification and mechanisms of cracking in welding high-alloy steels and nickel alloys in brittle temperature ranges. In: *Hot cracking phenomena in welds II*. Berlin; Heidelberg: Springer, 95–114.
13. Vallant, R., Cerjak, H. (2004) Investigation on the mechanical values and the hot crack susceptibility of Ni-base weld metals type 70/20 and 70/15 of different Nb contents. *IIW Doc. II-1535-04*.
14. Savage, W.F., Lundin, C.D. (1965) The Vareststraint test. *Welding J.*, **44**(10), 433–442.
15. Savchenko, V.S., Yushchenko, K.A. (1993) Mechanism of formation and ways of prevention of underbead cracks in welding of austenitic steels. *Avtomatich. Svarka*, **12**, 8–11.
16. Yushchenko, K.A., Savchenko, V.S., Chervyakov, N.O. et al. (2010) Probable mechanism of cracking of stable-austenitic welds caused by oxygen segregation. *The Paton Welding J.*, **5**, 5–9.
17. Trefilov, V.I., Majboroda, V.P., Firstov, S.A. et al. (1986) Investigation of influence of localised shear deformation on composition of surface steel fractured in vacuum. *Metallfizika*, **8**(3), 78–83.

## NEW BOOK

### (2011) **Welding and Allied Processes.**

A series of books and monographs on welding, cutting, surfacing, brazing, coating deposition and other processes of metal treatment.

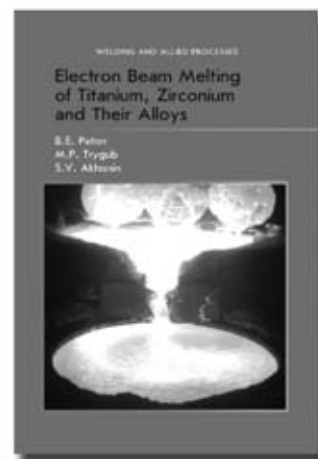
Edited by Prof. B.E. Paton, E.O. Paton Electric Welding Institute, NASU, Kyiv, Ukraine, 216 pp.

### **Electron Beam Melting of Titanium, Zirconium and Their Alloys**

B.E. Paton, M.P. Trygub and S.V. Akhonin

The book considers peculiarities of metallurgical production of titanium and zirconium ingots by the electron beam melting method. Mechanisms and patterns of behaviour of impurities, non-metallic inclusions and alloying elements during the EBM of titanium, zirconium and their alloys are detailed. Optimal technological parameters for melting of high-reactivity metals are suggested, providing high quality, technical and economic indices of this metallurgical process. Quality characteristics of the resulting ingots, including their chemical composition, micro- and macrostructure, as well as some mechanical properties of metal in the cast and wrought states, are given. Flow diagrams of melting and glazing of surfaces of the ingot are presented, and specific features of designs of electron beam units are described.

The book is meant for scientists, engineers and technicians, as well as for students of metallurgical departments of institutes of higher education.



Kindly send the orders for the book to the Editorial Board of «The Paton Welding Journal»

Phone/Fax: (38044) 200-82-77, e-mail: [journal@paton.kiev.ua](mailto:journal@paton.kiev.ua)